Supporting Information

Unconventional Formation of Cyanamide, a Key Intermediate in Prebiotic Chemical Evolution, in Interstellar Ice Analogues

Jia Wang,[1,2] Joshua H. Marks,[1,2] André K. Eckhardt,[3*] Ralf I. Kaiser[1,2*]

[1] *W. M. Keck Research Laboratory in Astrochemistry, University of Hawaii at Manoa, Honolulu, Hawaii 96822, United States*

[2] *Department of Chemistry, University of Hawaii at Manoa, Honolulu, Hawaii 96822, United States*

[3] *Lehrstuhl für Organische Chemie II, Ruhr-Universität Bochum, Bochum 44801, Germany*

[*]Corresponding Authors:

André K. Eckhardt, Andre.Eckhardt@ruhr-uni-bochum.de

Ralf I. Kaiser, ralfk@hawaii.edu

Methods

Experimental. All experiments were performed in an ultrahigh vacuum chamber maintained at pressures of a few 10^{-11} Torr using magnetically suspended turbomolecular pumps in combination with and an oil-free scroll pump; the experimetnal setup used in this work has been described previously.[1,2] A closed-cycle helium cryostat cooled a polished silver substrate to temperatures as low as 5 K and enabled vertical translation and horizontal rotation via an adjustable bellows and a rotatable flange, respectively.[1,2] The experiments utilized ammonia (NH_3; Matheson, 99.99%), ammonia-d_3 (ND_3; Sigma-Aldrich, 99% D), methylamine (CH_3NH_2; 99.5% Matheson TriGas), and methylamine-d_5 (CD_3ND_2; Cambridge Isotope Laboratories, 98% D). Once the substrate reached 5 K, the ice mixture was prepared by depositing ammonia and methylamine independently through separate glass capillary arrays at partial pressure of 1×10^{-8} Torr.[3] During deposition, the ice thickness was monitored *in situ* by laser interferometry through the recording interference fringes generated by a helium-neon laser (632.8 nm) reflected from both the silver substrate and the ice surface.[4] The thickness of NH_3–CH_3NH_2 ice was determined to be 700 ± 30 nm (Table S5) using an average refractive index (n) of 1.36 ± 0.04, calculated from the refractive indices of ammonia (n = 1.33 ± 0.01) and methylamine (n = 1.38 ± 0.01) ices at 18 K.[5] Fourier transform infrared (FTIR) spectra of NH_3–CH_3NH_2 and ND_3–CD_3ND_2 ice mixtures were collected using a Nicolet 6700 spectrometer (Thermo Electron) over 6000−500 cm^{-1} with 4 cm^{-1} resolution. The ratio of ammonia to methylamine in NH_3–CH_3NH_2 ice was determined to be 1.0 ± 0.5: 1 using integrated infrared absorptions of ν_2 mode at 1088 cm^{-1} (2.1×10^{-17} cm molecule^{-1}) for ammonia,[6] ν_6 mode at 1423 cm^{-1} (1.8×10^{-19} cm molecule^{-1}), the combined ν_5 and ν_{12} modes from 1433 to 1520 cm^{-1} (1.73×10^{-18} cm molecule^{-1}), the CH stretching region (ν_2, ν_3, and ν_{11}) spanning 2727–3015 cm^{-1} (2.3×10^{-17} cm molecule^{-1}) for methylamine.[5] Ice densities of 0.68 ± 0.01 g cm^{-3} for NH_3 ice and 0.732 ± 0.01 g cm^{-3} for CH_3NH_2 ice were used.[5]

After deposition, the ice mixtures were subjected to energetic electron irradiation using a 5 keV electron gun (SPECS, EQ PU-22) to simulate secondary electrons generated by GCRs as they penetrate interstellar ices in cold molecular cloud.[7,8] The ice mixtures were irradiated at an incidence angle of 70° with a beam current of 103 nA for 60 minutes (low dose) and 996 nA, 60 minutes (high dose) (Table S5). The low irradiation dose of 6.7 ± 1.0 eV ammonia^{-1} and 12 ± 2 eV methylamine^{-1} was calculated via Monte Carlo simulations with the CASINO software suite[9]

and corresponds to GCR exposure over molecular cloud lifetimes of $(3.9 \pm 0.6) \times 10^7$ years.[10] Monte Carlo simulations indicate an average penetration depth of 360 ± 40 nm for electrons in NH_3–CH_3NH_2 ice, with 99% of the electron energy deposited within the upper 560 ± 50 nm of the ice—well below the total thickness of 950 ± 50 nm—thus preventing electron–substrate interactions. Infrared spectra of the ices were collected *in situ* before, during, and after electron irradiation to monitor chemical evolution.

After irradiation, the ices were subjected to temperature-programmed desorption (TPD) by heating from 5 to 320 K at a rate of 1 K min^{-1}. Molecules desorbing into the gas phase during TPD were photoionized with pulsed (30 Hz) vacuum ultraviolet (VUV) light at 10.70, 10.35, and 10.40–10.61, which were generated via resonant four-wave mixing in a krypton gas jet through difference-frequency generation ($2\omega_1-\omega_2$). The laser beams (ω_1 and ω_2) were generated by two tunable dye laser (Sirah Lasertechnik, Cobra-Stretch) pumped by two Nd:YAG lasers (Spectra-Physics Quanta Ray PRO 270-30 and 250-30), with detailed VUV generation parameters provided in Table S6. The VUV light was separated from the fundamental beams (ω_1 and ω_2) using a biconvex lithium fluoride lens in an off-axis configuration and directed 2.0 ± 0.5 mm above the ice surface to ionize subliming molecules in the gas phase. The resulting ions were analyzed with a reflectron time-of-flight mass spectrometer (Jordan TOF Products) and detected using a dual microchannel plate detector. Ion signals processed through amplification and discrimination and recorded using a multichannel scaler (FAST ComTec, MCS6A). Each mass spectrum was acquired with a temporal resolution of 3.2 ns and was accumulated for 2 minutes (3600 sweeps).

Computational. All computations were conducted with Gaussian 16, Revision C.01.[11] In general, we used the density functional theory (DFT) B3LYP functional[12-14] in combination with the Dunning correlation consistent split valence basis set cc-pVTZ[15] for geometry optimizations and frequency calculations. The electronic energies based on these geometries were refined at the frozen-core coupled cluster[16-19] CCSD(T)/cc-pVTZ and CCSD(T)/cc-pVQZ level of theory and the obtained single point energies were extrapolated to the complete basis set limit[20-22] using ORCA 6.0.1.[23] The overall energy was obtained by correcting the electronic energies at the CCSD(T)/CBS level of theory with the zero-point vibrational energies (ZPVE) calculated at the B3LYP/aug-cc-pVTZ level of theory. The adiabatic ionization energies (IEs) were obtained by taking the ZPVE-corrected energy difference between radical cationic and neutral species of

similar conformations. The IE ranges are corrected for the combined error limits of −0.03/+0.06 eV[24] and the thermal and Stark effect by −0.03 eV (Table S4). Franck Condon factors were computed at the same B3LYP/aug-cc-pVTZ level of theory. Cartesian coordinates and harmonic frequencies are summarized in Table S7.

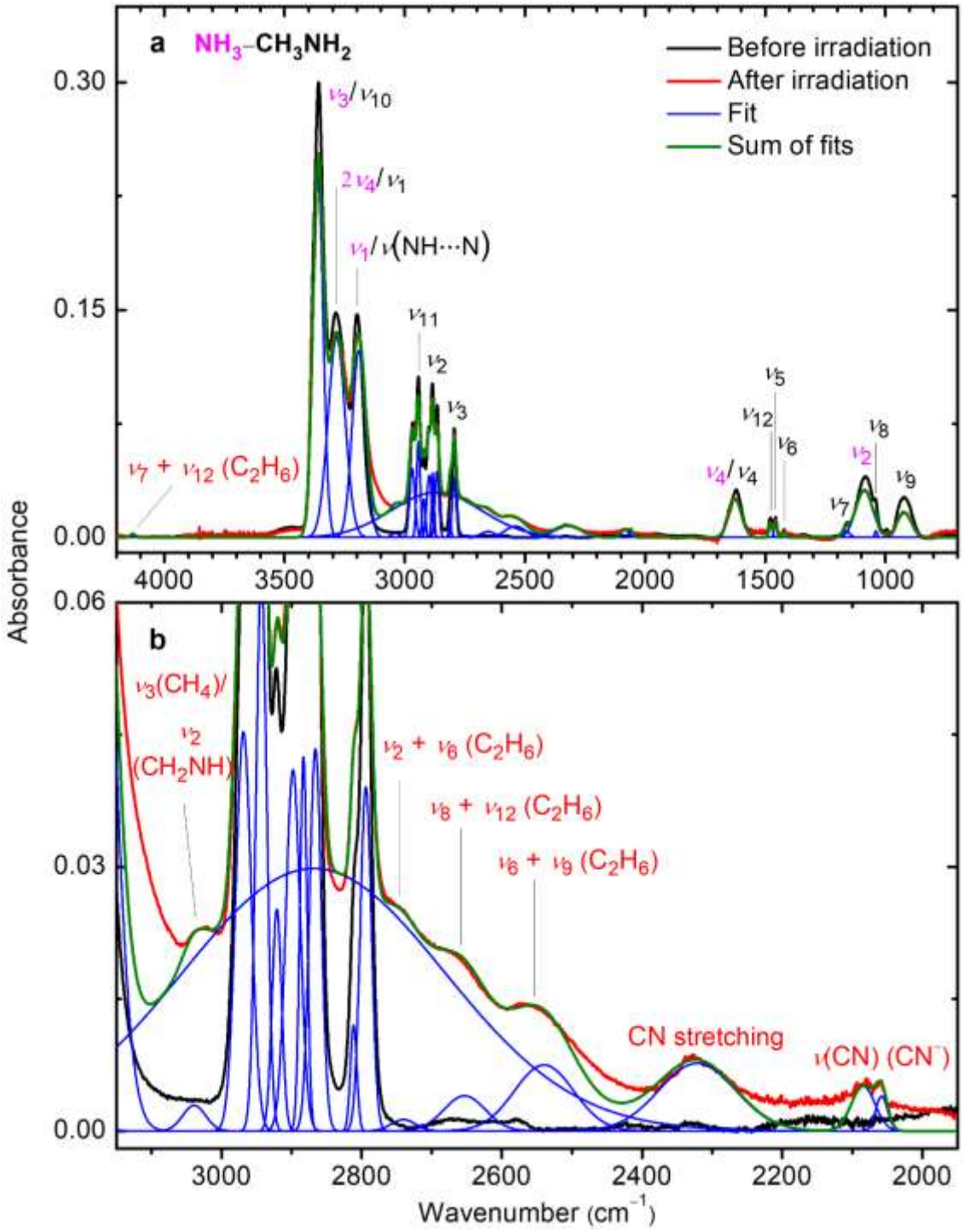

Figure S1. Infrared spectra of (a) NH_3–CH_3NH_2 ice recorded before and after low-dose irradiation (103 nA, 60 minutes) at 5 K, and (b) a magnified view with deconvolution of the 3150–1950 cm^{-1} region. Absorptions attributed to NH_3, CH_3NH_2, and new absorptions after irradiation are labeled in magenta, black, and red, respectively. Detailed assignments are provided in Table S1.

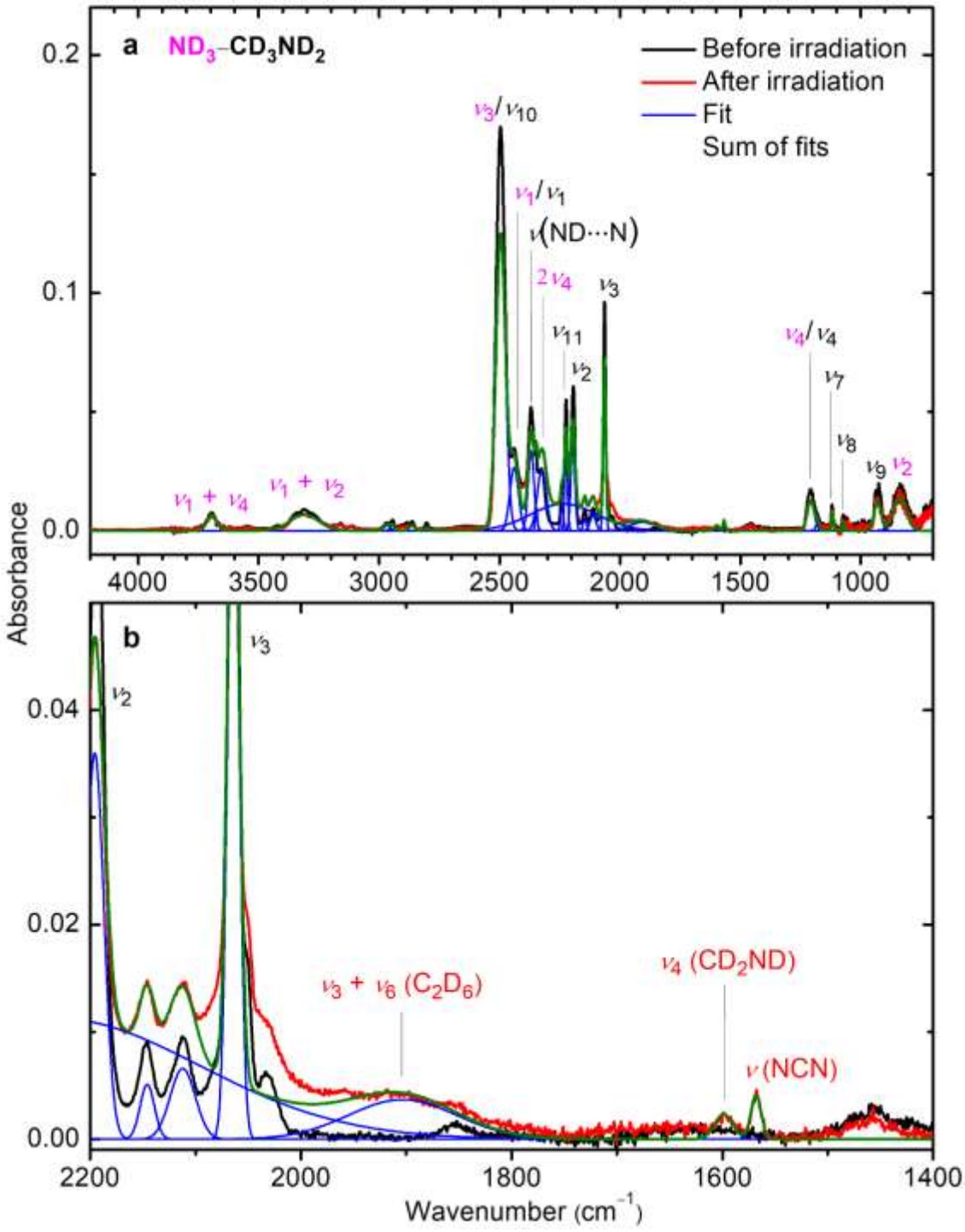

Figure S2. Infrared spectra of (a) ND_3–CD_3ND_2 ice recorded before and after low-dose irradiation (102 nA, 60 minutes) at 5 K, and (b) a magnified view with deconvolution of the 2200–1400 cm^{-1} region. Absorptions attributed to ND_3, CD_3ND_2, and new absorptions after irradiation are labeled in magenta, black, and red, respectively. Detailed assignments are provided in Table S2.

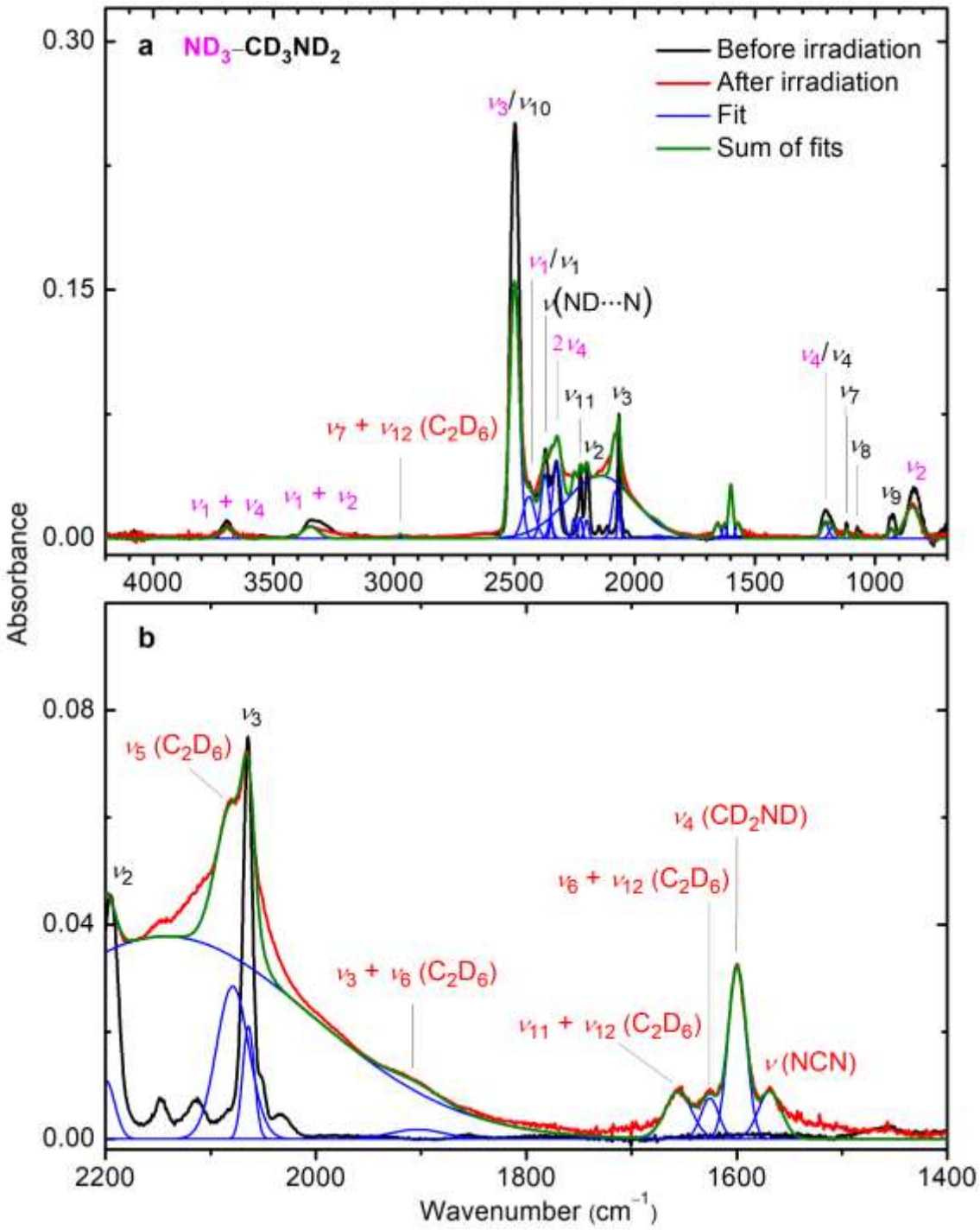

Figure S3. Infrared spectra of (a) ND_3–CD_3ND_2 ice recorded before and after high-dose irradiation (972 nA, 60 minutes) at 5 K, and (b) a magnified view with deconvolution of the 2200–1400 cm^{-1} region. Absorptions attributed to ND_3, CD_3ND_2, and new absorptions after irradiation are labeled in magenta, black, and red, respectively. Detailed assignments are provided in Table S3.

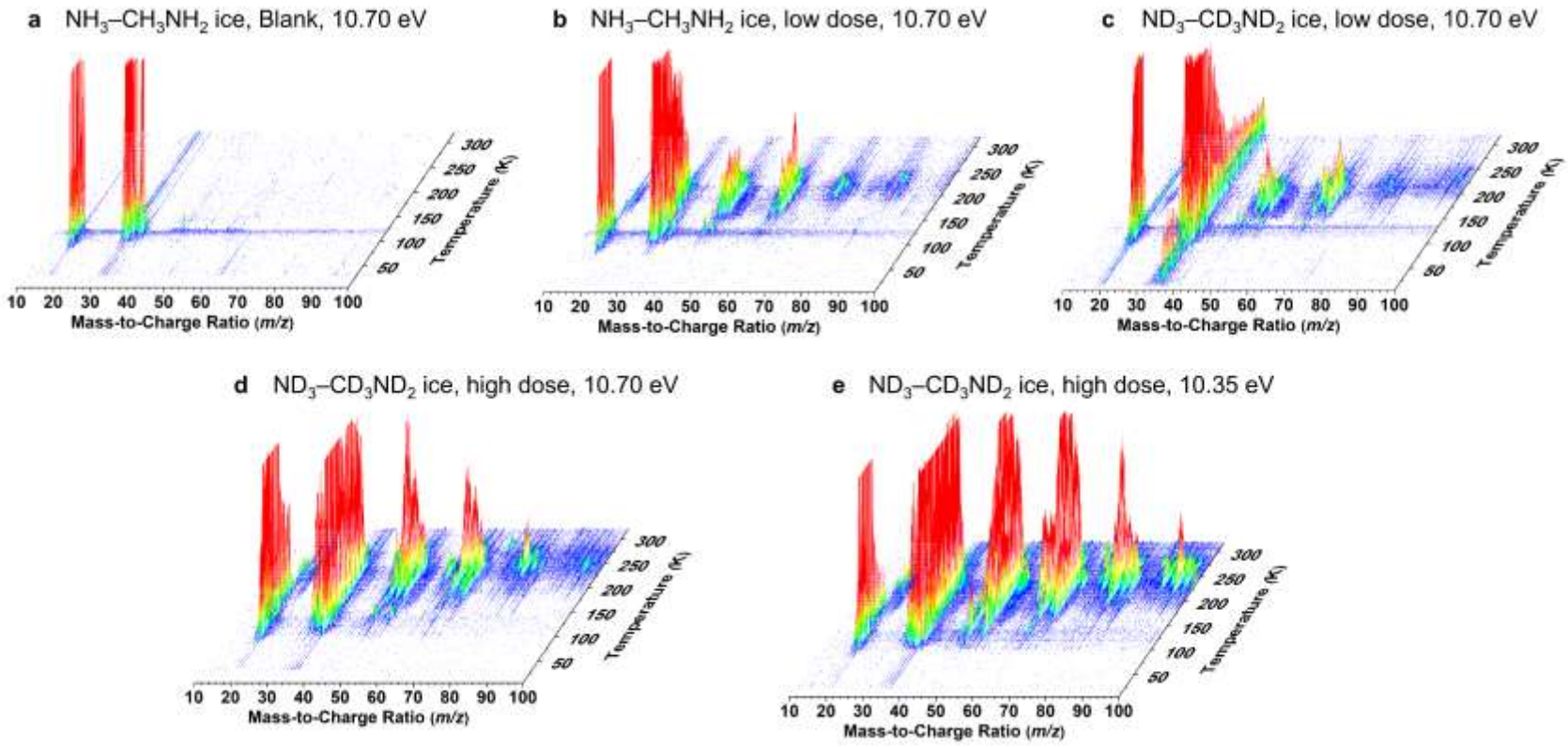

Figure S4. PI-ReToF-MS data of ammonia–methylamine ices during TPD. Data were recorded at 10.70 eV for the blank (unirradiated) NH_3–CH_3NH_2 ice (a), low-dose irradiated NH_3–CH_3NH_2 ice (b) and ND_3–CD_3ND_2 ice at 10.70 eV (c), and high-dose irradiated ND_3–CD_3ND_2 ice recorded at 10.70 eV (d) and 10.35 eV (e).

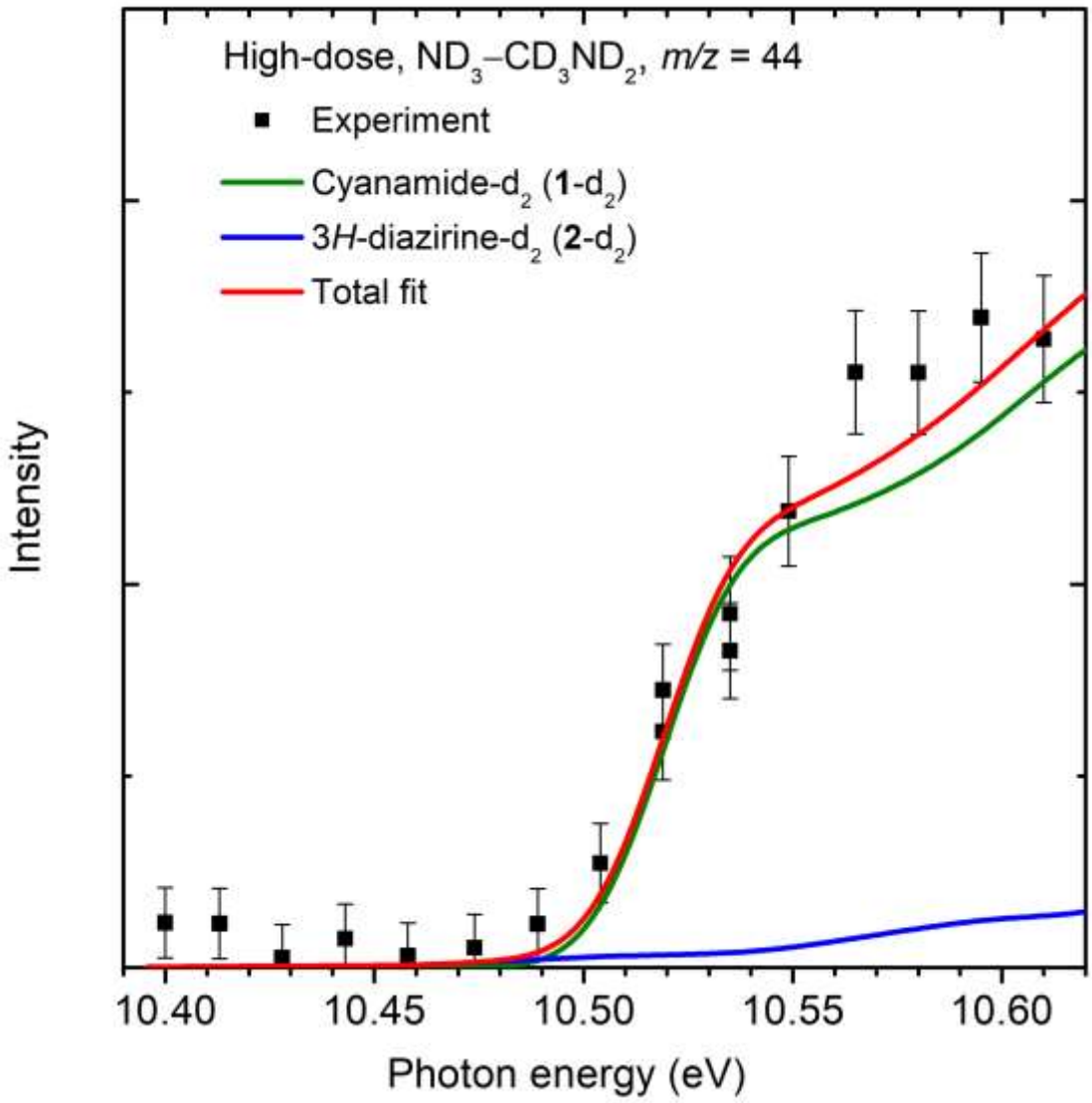

Figure S5. Photoionization efficiency (PIE) curve of *m/z* = 44 collected during TPD between 237 and 255 K after correction for temperature-dependent sublimation rate. Fitting the experimental data with simulated Franck–Condon PIE curves of cyanamide-d_2 (**1**-d_2) and 3*H*-diazirine-d_2 (**2**-d_2) shows that up to 7% of the total ion signal can be attributed to **2**-d_2, indicating its tentative assignment.

Table S1. Observed absorption peaks of NH_3–CH_3NH_2 ice before and after irradiation (103 nA, 60 minutes) at 5 K.

Infrared absorptions before irradiation (cm^{-1})	
NH_3	Assignment[3,6]
4995	$\nu_1 + \nu_4$
4474	$\nu_1 + \nu_2$
3356	ν_3
3284	$2\nu_4$
3191	ν_1
1626	ν_4
1088	ν_2
CH_3NH_2	Assignment[3,25,26]
4948	$\nu_1 + \nu_4$
3356	ν_{10}
3284	ν_1
3191	ν(NH) H-bonding
2943	ν_{11}
2883	ν_2
2794	ν_3
2969	$2\nu_{12}$
2921	$\nu_5 + \nu_{12}$
2898	$2\nu_5$
2812	$\nu_4 + \nu_7$
1626	ν_4
1478	ν_{12}
1458	ν_5
1423	ν_6
1164	ν_7
1040	ν_8
923	ν_9
New infrared absorptions after irradiation (cm^{-1})	Assignment
4132	$\nu_7 + \nu_{12}$ (C_2H_6)[27]
3039	ν_3 (CH_4)[28] / ν_2 (CH_2NH)[29]
2869	C–H stretching[27,30]
2740	$\nu_2 + \nu_6$ (C_2H_6)[27]
2653	$\nu_8 + \nu_{12}$ (C_2H_6)[27]
2540	$\nu_6 + \nu_9$ (C_2H_6)[27]
2321	C≡N stretching[30]
2085, 2058	ν(C≡N) (CN^-)[31]

Table S2. Observed absorption peaks of ND_3–CD_3ND_2 ice before and after irradiation (102 nA, 60 minutes) at 5 K.

Infrared absorptions before irradiation (cm^{-1})	
ND_3	Assignment[3]
4809	$2\nu_1 + \nu_4$
3696	$\nu_1 + \nu_4$
3311	$\nu_1 + \nu_2$
2495	ν_3
2439	ν_1
2325	$2\nu_4$
1180	ν_4
838	ν_2
CD_3ND_2	Assignment[3,25]
4809	$2\nu_1$
2968	$\nu_3 + \nu_9$
2943	ν_{11} (CH_3NH_2)
2864	ν_2 (CH_3NH_2)
2803	ν_3 (CH_3NH_2)
2495	ν_{10}
2439	ν_1
2369	ν(ND) H-bonding
2347	$\nu_4 + \nu_{11}$
2240	$2\nu_7$
2224	ν_{11}
2196	ν_2
2064	ν_3
1208	ν_4
1118	ν_7
1073	ν_8
930	ν_9
New infrared absorptions after irradiation (cm^{-1})	Assignment
2234	CD stretching
1904	$\nu_3 + \nu_6$ (C_2D_6)[27]
1599	ν_4 (CD_2ND)[29]
1568	ν(NCN)[32]

Table S3. Observed absorption peaks of ND_3–CD_3ND_2 ice before and after high-dose irradiation (972 nA, 60 minutes) at 5 K.

Infrared absorptions before irradiation (cm^{-1})	
ND_3	Assignment[3]
4814	$2\nu_1 + \nu_4$
3695	$\nu_1 + \nu_4$
3347	$\nu_1 + \nu_2$
2499	ν_3
2439	ν_1
2323	$2\nu_4$
1179	ν_4
846	ν_2
CD_3ND_2	Assignment[3,25]
4814	$2\nu_1$
2973	$\nu_3 + \nu_9$
2499	ν_{10}
2439	ν_1
2371	ν(ND) H-bonding
2347	$\nu_4 + \nu_{11}$
2250	$2\nu_7$
2225	ν_{11}
2200	ν_2
2064	ν_3
1208	ν_4
1119	ν_7
1074	ν_8
933	ν_9
New infrared absorptions after irradiation (cm^{-1})	Assignment
2973	$\nu_7 + \nu_{12}$ (C_2D_6)[27]
2143	CD stretching
2079	ν_5 (C_2D_6)[27]
1904	$\nu_3 + \nu_6$ (C_2D_6)[27]
1655	$\nu_{11} + \nu_{12}$ (C_2D_6)[27]
1626	$\nu_6 + \nu_{12}$ (C_2D_6)[27]
1600	ν_4 (CD_2ND)[29]
1569	ν(NCN)[32]

Table S4. Error analysis of adiabatic ionization energies (IEs) and relative energies (ΔE) of CH_2N_2 isomers calculated at the CCSD(T)/CBS//B3LYP/aug-cc-pVTZ level of theory including the zero-point vibrational energy (ZPVE) corrections. The IE ranges are corrected for the combined error limits of −0.03/+0.06 eV[24] and the thermal and Stark effect by −0.03 eV.

Isomers	Structure	ΔE (kJ mol^{-1})	Computed IE (eV)	Corrected IE ranges (eV)
1 Cyanamide	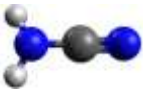	0	10.58	10.52–10.61
2 3*H*-Diazirine	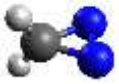	178	10.43	10.37–10.46
3 Isocyanamide	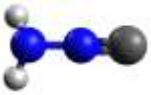	186	10.29	10.23–10.32
4 Methanediimine	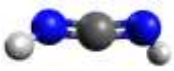	11	10.24	10.18–10.27
5 1*H*-Diazirine		63	9.63	9.57–9.66
6 Methyl, 2-hydrazinyl-1-ylidene-		236	9.08	9.02–9.11
7 Diazomethane	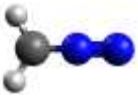	32	9.00	8.94–9.03

Table S5. Experimental parameters of ammonia–methylamine ices: ice composition, ratio, thickness, irradiation current and time, and photon energy.

Ice composition	Ratio of ammonia to methylamine	Thickness (nm)	Current (nA)	Irradiation time (s)	Dose (eV/ ammonia)	Dose (eV/ methylamine)	Photon energy (eV)
NH_3–CH_3NH_2	0.9 ± 0.5 : 1	700 ± 30	–	–	–	–	10.70
NH_3–CH_3NH_2	0.5 ± 0.3 : 1	700 ± 30	103 ± 2	3600 ± 10	6.7 ± 1.0	12 ± 2	10.70
ND_3–CD_3ND_2	0.4 ± 0.1 : 1	700 ± 30	102 ± 1	3600 ± 10	7.7 ± 1.2	14 ± 2	10.70
ND_3–CD_3ND_2	0.9 ± 0.2 : 1	700 ± 30	996 ± 10	3600 ± 10	76 ± 12	135 ± 21	10.70
ND_3–CD_3ND_2	1.0 ± 0.2 : 1	700 ± 30	972 ± 10	3600 ± 10	74 ± 11	132 ± 20	10.35
ND_3–CD_3ND_2	1.4 ± 0.5 : 1	720 ± 40	1025 ± 10	3600 ± 10	78 ± 12	139 ± 21	10.40–10.54
ND_3–CD_3ND_2	1.1 ± 0.3 : 1	750 ± 40	1005 ± 10	3600 ± 10	76 ± 12	137 ± 21	10.52–10.61

Table S6. Parameters for generating vacuum ultraviolet (VUV) light, with the photon energy uncertainty of less than 0.001 eV.

VUV photon energy (eV) ($2\omega_1-\omega_2$)	Nonlinear medium in four-wave mixing	Laser wavelength for ω_1 (nm)	Dye for ω_1	Laser wavelength for ω_2 (nm)	Dye for ω_2
10.70	Krypton	202.316	Rhodamine 610 and 640	796.573	LDS 798
10.52–10.61	Krypton	202.316	Rhodamine 610 and 640	714–753	LDS 751
10.40–10.54	Krypton	202.316	Rhodamine 610 and 640	667–722	LDS 698
10.35	Krypton	202.316	Rhodamine 610 and 640	650.334	Rhodamine 640

Table S7. Optimized Cartesian coordinates (distances in Å), electronic energies (in hartree), harmonic frequencies (cm^{-1}), and infrared intensities (km mol^{-1}) of CH_2N_2 isomers calculated at B3LYP/aug-cc-pVTZ level of theory.

1

N	1.192742	–0.009308	–0.000000
C	–0.147453	–0.001016	0.000000
H	1.625330	–0.354866	–0.843507
H	1.625330	–0.354866	0.843507
N	–1.300337	0.061259	0.000000

E = –148.8486067
E[CCSD(T)/CBS] = –148.6218664
ZPVE = 21.3255 kcal mol^{-1}

Frequency	**Intensity**
411.5221	0.2169
489.7130	79.3987
563.8031	141.7468
1093.7343	10.0069
1194.3711	0.0390
1632.5373	39.2154
2350.3298	118.4330
3545.7901	40.0852
3635.6087	65.8218

1 radical cation

N	1.134508	–0.202112	–0.000000
C	–0.134290	–0.035812	0.000000
H	1.655212	–0.270493	–0.879711
H	1.655212	–0.270493	0.879711
N	–1.313994	0.118733	0.000000

E = –148.4666977
E[CCSD(T)/CBS] = –148.2320102
ZPVE = 20.5533 kcal mol^{-1}

Frequency	**Intensity**
379.4516	0.8966
409.9781	0.4718
759.3035	186.8130
1126.7964	3.7895
1183.8209	0.7914
1601.7577	80.4213
2063.5870	69.8052
3378.5865	300.8298
3473.9556	273.7512

2

N	0.000000	–0.607674	0.475872
N	–0.000000	0.607674	0.475872
C	0.000000	–0.000000	–0.872672
H	0.931848	0.000000	–1.416551
H	–0.931848	–0.000000	–1.416551

E = –148.7759796
E[CCSD(T)/CBS] = –148.5532859
ZPVE = 20.8699 kcal mol^{-1}

Frequency	**Intensity**
827.6801	14.0601
988.2258	0.0000
1002.7159	32.6710
1025.6857	4.2675
1144.6669	3.7669
1499.3441	3.1667

2 radical cation

N	–0.000000	0.534480	–0.521510
N	0.000000	–0.597988	–0.687787
C	–0.000000	0.071502	0.933342
H	0.977205	–0.009838	1.388629
H	–0.977205	–0.009838	1.388629

E = –148.3944089
E[CCSD(T)/CBS] = –148.1668715
ZPVE = 18.8910 kcal mol^{-1}

Frequency	Intensity
224.1791	4.1822
509.5657	0.0107
674.7281	12.5296
878.0015	31.1768
1067.3884	3.2289
1404.3983	12.1320

1730.6800	23.1397			2012.4778	22.3882		
3132.6337	6.1645			3127.9804	42.8812		
3247.0452	9.4391			3315.7052	75.2802		
3				**3 radical cation**			
N	1.154127	0.010092	–0.000000	N	1.058215	–0.263142	–0.000000
N	–0.200442	–0.014110	0.000000	N	–0.186828	–0.048893	0.000000
H	1.496798	–0.463085	–0.828831	H	1.551752	–0.348026	–0.894629
H	1.496798	–0.463085	0.828831	H	1.551752	–0.348026	0.894629
C	–1.364295	0.082473	0.000000	C	–1.379951	0.155752	0.000000
E = –148.7779304				E = –148.4049327			
E[CCSD(T)/CBS] = –148.5505730				E[CCSD(T)/CBS] = –148.1704840			
ZPVE = 21.1217 kcal mol^{-1}				ZPVE = 19.9534 kcal mol^{-1}			
Frequency	**Intensity**			**Frequency**	**Intensity**		
265.2047	1.3549			175.4666	0.5911		
352.4071	5.3779			200.5967	13.5137		
844.4880	123.4833			680.8759	159.9760		
1053.5386	20.4404			1184.4584	5.7116		
1342.8954	4.3799			1235.4504	0.3794		
1659.9976	20.8101			1629.3049	49.6841		
2217.9883	33.3598			2020.0144	329.4370		
3475.3431	10.6086			3352.5758	217.4749		
3562.9747	30.3254			3478.8618	238.6257		
4				**4 radical cation**			
C	0.000198	–0.017909	–0.001709	C	–0.000000	0.000000	0.083712
N	–1.210768	0.085927	–0.094204	N	1.200028	–0.000000	–0.075291
N	1.210975	0.071883	0.106055	N	–1.200028	0.000000	–0.075291
H	1.815238	–0.464925	–0.499808	H	–2.006664	0.000000	0.547749
H	–1.814131	–0.533026	0.428497	H	2.006664	–0.000000	0.547749
E = –148.8497725				E = –148.4734161			
E[CCSD(T)/CBS] = –148.6162695				E[CCSD(T)/CBS] = –148.2364167			
ZPVE = 20.4910 kcal mol^{-1}				ZPVE = 18.1807 kcal mol^{-1}			
Frequency	**Intensity**			**Frequency**	**Intensity**		
545.1149	0.4443			222.7380	351.8951		
548.9176	72.7798			471.8782	13.1116		
715.7462	89.5040			517.2969	28.5769		
916.9507	441.9046			592.9679	0.0000		
918.5857	14.6197			760.4516	109.7934		
1288.0138	0.0000			1318.4123	0.1256		
2216.4862	703.4179			1805.2224	8.9475		
3590.3990	147.2469			3504.3791	705.5516		

3593.4584 23.8482	3524.2359 150.0997
5	**5 radical cation**
C 0.362980 –0.561586 0.013773 N –0.898836 0.042220 –0.141371 N 0.661869 0.635767 0.010304 H –1.310940 0.163292 0.787038 H 0.805118 –1.547128 0.056993 E = –148.7444342 E[CCSD(T)/CBS] = –148.5206107 ZPVE = 20.3922 kcal mol^{-1} Frequency Intensity 548.0821 7.7608 817.4672 24.4000 966.1262 56.0518 1035.4545 18.7495 1178.2445 30.2507 1344.9800 12.2867 1789.6795 6.9539 3204.4846 1.2572 3380.0050 1.7673	C 0.402673 –0.621817 –0.005229 N –0.726566 0.051150 0.073270 N 0.599151 0.660612 –0.039214 H –1.505893 0.252954 0.710601 H 0.850827 –1.610335 –0.012690 E = –148.3942772 E[CCSD(T)/CBS] = –148.1652085 ZPVE = 19.5208 kcal mol^{-1} Frequency Intensity 601.0120 100.2491 756.8742 65.7025 879.9409 52.4801 958.5678 25.4798 994.7045 5.7754 1221.6355 16.2919 1632.1169 27.2374 3210.8774 110.9954 3399.2376 298.2043
6	**6 radical cation**
N 0.271502 –1.115568 0.073407 N –0.025194 0.081571 –0.024001 C –0.461331 1.161709 –0.248514 H 1.285438 –1.225761 0.024303 H –0.701095 1.993220 0.387868 E = –148.7640902 E[CCSD(T)/CBS] = –148.5295357 ZPVE = 19.8592 kcal mol^{-1} **Frequency** **Intensity** 475.0401 8.9772 529.5602 116.8626 646.9055 283.3073 839.1999 40.2271 1246.2942 118.4964 1319.3475 54.5182 2126.2701 421.2551 3290.3256 51.9843 3418.7885 14.0301	N –1.176243 –0.090731 –0.000000 N 0.081251 0.054106 –0.000000 C 1.234581 –0.014317 0.000000 H –1.647936 0.829678 –0.000000 H 2.311445 –0.049892 0.000000 E = –148.4296348 E[CCSD(T)/CBS] = –148.1943337 ZPVE = 18.8538 kcal mol^{-1} Frequency Intensity 421.8955 33.3892 436.6575 26.3120 624.0977 44.9530 646.6780 22.7624 1045.8051 85.0470 1288.9587 74.9042 2084.0177 3.9990 3310.1024 420.3964 3330.1860 63.9670

7

N	–0.000000	0.000000	1.287561
N	–0.000000	–0.000000	0.155450
C	0.000000	0.000000	–1.136620
H	0.000000	0.950107	–1.640680
H	–0.000000	–0.950107	–1.640680

E = –148.8015772
E[CCSD(T)/CBS] = –148.5682504
ZPVE = 19.8652 kcal mol^{-1}

Frequency	**Intensity**
429.6356	0.2021
438.1438	127.1371
581.1458	7.9300
1116.9036	2.3631
1208.8382	4.9737
1439.8783	35.8292
2190.8264	446.9922
3184.9355	14.1755
3305.5990	2.7494

7 radical cation

N	–0.000000	–0.000000	1.291807
N	–0.000000	–0.000000	0.179451
C	0.000000	0.000000	–1.154312
H	0.000000	0.966573	–1.645958
H	–0.000000	–0.966573	–1.645958

E = –148.4679643
E[CCSD(T)/CBS] = –148.2368420
ZPVE = 19.5092 kcal mol^{-1}

Frequency	**Intensity**
386.6022	0.9245
434.8546	0.4029
747.7559	44.6997
1051.2604	0.2939
1111.6317	3.1503
1401.7917	31.1897
2150.5166	25.4517
3107.9938	97.4798
3254.4665	88.7894

Supplementary References

(1) Abplanalp, M. J.; Forstel, M.; Kaiser, R. I. Exploiting single photon vacuum ultraviolet photoionization to unravel the synthesis of complex organic molecules in interstellar ices. *Chem. Phys. Lett.* **2016**, *644*, 79-98.
(2) Wang, J.; Zhang, C.; Marks, J. H.; Evseev, M. M.; Kuznetsov, O. V.; Antonov, I. O.; Kaiser, R. I. Interstellar formation of lactaldehyde, a key intermediate in the methylglyoxal pathway. *Nat. Commun.* **2024**, *15*, 10189.
(3) Marks, J. H.; Wang, J.; Fortenberry, R. C.; Kaiser, R. I. Preparation of methanediamine ($CH_2(NH_2)_2$—A precursor to nucleobases in the interstellar medium. *Proc. Natl. Acad. Sci. U.S.A.* **2022**, *119*, e2217329119.
(4) Turner, A. M.; Abplanalp, M. J.; Chen, S. Y.; Chen, Y. T.; Chang, A. H. H.; Kaiser, R. I. A photoionization mass spectroscopic study on the formation of phosphanes in low temperature phosphine ices. *Phys. Chem. Chem. Phys.* **2015**, *17*, 27281-27291.
(5) Hudson, R. L.; Yarnall, Y. Y.; Gerakines, P. A. Infrared spectral intensities of amine ices, precursors to amino acids. *Astrobiology* **2022**, *22*, 452-461.
(6) Bouilloud, M.; Fray, N.; Benilan, Y.; Cottin, H.; Gazeau, M. C.; Jolly, A. Bibliographic review and new measurements of the infrared band strengths of pure molecules at 25 K: H_2O, CO_2, CO, CH_4, NH_3, CH_3OH, HCOOH and H_2CO. *Mon. Not. R. Astron. Soc.* **2015**, *451*, 2145-2160.
(7) Kaiser, R. I.; Roessler, K. Theoretical and laboratory studies on the interaction of cosmic-ray particles with interstellar ices. I. Synthesis of polycyclic aromatic hydrocarbons by a cosmic-ray-induced multicenter mechanism. *Astrophys. J.* **1997**, *475*, 144.
(8) Ferrari, B. C.; Slavicinska, K.; Bennett, C. J. Role of suprathermal chemistry on the evolution of carbon oxides and organics within interstellar and cometary ices. *Acc. Chem. Res.* **2021**, *54*, 1067-1079.
(9) Drouin, D.; Couture, A. R.; Joly, D.; Tastet, X.; Aimez, V.; Gauvin, R. CASINO V2.42 - A fast and easy-to-use modeling tool for scanning electron microscopy and microanalysis users. *Scanning* **2007**, *29*, 92-101.
(10) Yeghikyan, A. G. Irradiation of dust in molecular clouds. II. Doses produced by cosmic rays. *Astrophysics* **2011**, *54*, 87-99.
(11) M. J. Frisch, G. W. T., H. B. Schlegel, G. E. Scuseria, M. A. Robb, J. R. Cheeseman, G. Scalmani, V. Barone, G. A. Petersson, H. Nakatsuji, et al. Gaussian 09, Revision D. 01; Gaussian: Wallingford, CT, USA. **2009**.
(12) Becke, A. D. Density-functional exchange-energy: Approximation with correct asymptotic behavior. *Phys. Rev. A* **1988**, *38*, 3098-3100.
(13) Lee, C.; Yang, W.; Parr, R. G. Development of the Colle-Salvetti correlation-energy formula into a functional of the electron density. *Phys. Rev. B* **1988**, *37*, 785-789.
(14) Becke, A. D. Density-functional thermochemistry. III. The role of exact exchange. *J. Chem. Phys.* **1993**, *98*, 5648-5652.
(15) Dunning, T. H. Gaussian basis sets for use in correlated molecular calculations. I. The atoms boron through neon and hydrogen. *J. Chem. Phys.* **1989**, *90*, 1007-1023.
(16) Čížek, J. On the correlation problem in atomic and molecular systems. Calculation of wavefunction components in ursell-type expansion using quantum-field theoretical methods. *J. Chem. Phys.* **1966**, *45*, 4256-4266.
(17) Bartlett, R. J.; Watts, J. D.; Kucharski, S. A.; Noga, J. Non-iterative fifth-order triple and quadruple excitation energy corrections in correlated methods. *Chem. Phys. Lett.* **1990**, *165*, 513-522.

(18) Raghavachari, K. Electron correlation techniques in quantum chemistry: Recent advances. *Annu. Rev. Phys. Chem.* **1991**, *42*, 615-642.
(19) Stanton, J. F. Why CCSD(T) works: a different perspective. *Chem. Phys. Lett.* **1997**, *281*, 130-134.
(20) Helgaker, T.; Klopper, W.; Koch, H.; Noga, J. Basis-set convergence of correlated calculations on water. *J. Chem. Phys.* **1997**, *106*, 9639-9646.
(21) Halkier, A.; Helgaker, T.; Jørgensen, P.; Klopper, W.; Koch, H.; Olsen, J.; Wilson, A. K. Basis-set convergence in correlated calculations on Ne, N_2, and H_2O. *Chem. Phys. Lett.* **1998**, *286*, 243-252.
(22) Zhong, S.; Barnes, E. C.; Petersson, G. A. Uniformly convergent n-tuple-ζ augmented polarized (nZaP) basis sets for complete basis set extrapolations. I. Self-consistent field energies. *J. Chem. Phys.* **2008**, *129*, 184116.
(23) Neese, F. Software update: The ORCA program system, version 4.0. *WIREs Comput. Mol. Sci.* **2018**, *8*, e1327.
(24) Wang, J.; Sun, B.-J.; Bergantini, A.; Wang, Z.; Turner, A. M.; Chang, A. H. H.; Kaiser, R. I. Interstellar formation of the elusive phosphanyloxyphosphane (H_2POPH_2) and phosphanylphosphinous acid (H_2PPHOH) via nonequilibrium chemistry: Precursors to the phosphate backbone of nucleotides. *J. Am. Chem. Soc.* **2025**, *147*, 38987-38991.
(25) Durig, J. R.; Bush, S. F.; Baglin, F. G. Infrared and raman investigation of condensed phases of methylamine and its deuterium derivatives. *J. Chem. Phys.* **1968**, *49*, 2106-2117.
(26) Zhu, C.; Frigge, R.; Turner, A. M.; Abplanalp, M. J.; Sun, B.-J.; Chen, Y.-L.; Chang, A. H.; Kaiser, R. I. A vacuum ultraviolet photoionization study on the formation of methanimine (CH_2NH) and ethylenediamine ($NH_2CH_2CH_2NH_2$) in low temperature interstellar model ices exposed to ionizing radiation. *Phys. Chem. Chem. Phys.* **2019**, *21*, 1952-1962.
(27) Abplanalp, M. J.; Kaiser, R. I. Complex hydrocarbon chemistry in interstellar and solar system ices revealed: A combined infrared spectroscopy and reflectron time-of-flight mass spectrometry analysis of ethane (C_2H_6) and D6-ethane (C_2D_6) ices exposed to ionizing radiation. *Astrophys. J.* **2016**, *827*, 132.
(28) Maity, S.; Kaiser, R. I.; Jones, B. M. Formation of ketene (H_2CCO) in interstellar analogous methane (CH_4)-carbon monoxide (CO) ices: A combined FTIR and reflectron time-of-flight mass spectroscopic study. *Astrophys. J.* **2014**, *789*, 36.
(29) Jacox, M. E.; Milligan, D. E. The infrared spectrum of methylenimine. *J. Mol. Spectrosc.* **1975**, *56*, 333-356.
(30) Socrates, G. *Infrared and raman characteristic group frequencies: Tables and charts*; John Wiley & Sons, Ltd., 2004.
(31) Gerakines, P. A.; Moore, M. H.; Hudson, R. L. Ultraviolet photolysis and proton irradiation of astrophysical ice analogs containing hydrogen cyanide. *Icarus* **2004**, *170*, 202-213.
(32) Davies, M.; Jones, W. J. The infra-red spectrum and structure of cyanamide and dimethylcyanamide. *Trans. Faraday Soc.* **1958**, *54*, 1454-1463.